DESIGN OF A MAJOR CO_2 FLOOD, NORTH WARD ESTES FIELD, WARD COUNTY, TEXAS*

R. Winzinger, J.L. Brink, and K.S. Patel, Chevron U.S.A. Inc.; C.B. Davenport, Cabinda Gulf Oil Co. Ltd.; and Y.R. Patel and G.C. Thakur, Chevron U.S.A. Inc.

ABSTRACT

The reservoir engineering aspects of the design of a major West Texas CO_2 flood are presented. The design included (1) a detailed fieldwide geologic study to characterize the principal Yates reservoirs, (2) a CO_2 injectivity test to identify any reduction in injectivity either during or following CO_2 injection, (3) laboratory work including oil-CO_2 phase behavior, slim tube tests with pure and contaminated CO_2 and corefloods to determine recovery of waterflood residual oil by CO_2 flooding, (4) reservoir simulation to predict flood performance. A comprehensive waterflood evaluation proceeded the selection of average pattern models for reservoir simulation. These three-dimensional models, which have up to twelve layers each, were history matched over the 33 year waterflood period. Predictions were made for continuation of the waterflood and for CO_2 flooding. Additional reservoir simulation was conducted to determine the optimum economic CO_2 slug size and to study the differences in recovery efficiency between line drives and five spots. Scale-up procedures were developed to predict from the average patterns the incremental oil production for the 3840 acre project area. It is predicted that CO_2 flooding will recover an additional 8% of the original oil in place (OOIP). The optimum CO_2 slug size lies between 38% to 60% hydrocarbon pore volume (HCPV). The optimum water-alternating-gas (WAG) ratio is 1:1. Gross and net CO_2 utilization ratios are 12 and 4 MSCF/STB (2136 and 712 m^3/m^3), respectively.

INTRODUCTION

The North Ward Estes (NWE) Field, located in Ward and Winkler Counties, Texas (Figure 1), was discovered in 1929. Cumulative oil produced is over 320 million barrels ($50.9 \times 10^6 m^3$) or about 25% OOIP. The field has been waterflooded since 1955.

Geologically, the NWE Field resides on the western flank of the Central Basin Platform. The Yates, the dominant producing formation, is composed of up to seven major reservoirs, composed of very fine grained sandstones to siltstones separated by dense dolomite beds. Within the 3840 acre (15.7 km^2) CO_2 project area, average depth is 2600 feet (792 m), porosity and permeability average 16% pore volume (PV) and 37 md ($37 \times 10^{-15} m^2$), respectively. Reservoir temperature is 83°F (28°C). The flood patterns are 20 acre ($81 \times 10^3 m^2$) five spots and line drives.

In early 1989, CO_2 flooding has been implemented in a six section (15.7 km^2) project area which is located in the better parts of the field in

* This paper (SPE 19654) was prepared for presentation at the 64th Annual Technical Conference and Exhibition of the Society of Petroleum Engineers held in San Antonio, Texas, October 8-11, 1989.

terms of cumulative oil production and reservoir rock quality. This paper, after a review of the field history and reservoir geology, will focus on the reservoir engineering aspects of the design of this CO_2 flood: laboratory work, CO_2 injectivity test and CO_2 flood performance predictions.

FIELD HISTORY AND DEVELOPMENT

The discovery and development of the North Ward Estes Field occurred with the completion of Gulf Oil Corporation's G. W. O'Brien No. 4 in April 1929. The field was initially developed on twenty acre spacing; the most productive parts of the field were drilled on ten acre spacing.

Until the early fifties, a typical completion consisted of: set 9 5/8 inch (24.5 cm) surface casing at a depth of 500-800 feet (152-244 m); drill to the top of the Yates; drill ahead and check for gas caps; set 7 inch (17.8 cm) casing through the gas sands; drill to total depth; shoot the producing section with nitroglycerine; clean out the hole and hang a 5½ inch (14 cm) perforated liner from the casing.

Completion practices changed in the early fifties to cased hole completions and use of hydraulic fracturing and acidizing as stimulation techniques. About half of the current producers and injectors are shot, open hole completions. Vertical sweep has been adversely affected because of the inability to measure and control the injection profiles in the shot, open hole injectors.

The production and injection history of the six section CO_2 flood project area is shown in Figure 2. Primary production peaked in 1944 and was approaching the economic limit in the mid-fifties. A pilot waterflood was started in 1954 on 960 acres (3.9 km^2) in the western halves of Sections 6, 7 and 8. Oil production responded very quickly and the flood was expanded to the rest of Sections 6 to 10 in 1955 and 1956. Twenty-seven additional wells were drilled to complete the initial waterflood patterns in these five sections. Except for parts of Sections 6, 7 and 8 which were developed on 20 acre (81 x $10^3 m^2$) five spots, the prevailing flood patterns were 40 acre (162 x $10^3 m^2$) five spots. Oil production increased steadily for the next five years until secondary production peaked in 1960.

In 1963, Section 3 was put on waterflood (40 acre (162 x $10^3 m^2$) five spot patterns). In 1968, sixty additional infill wells were drilled and, in order to reduce the well spacing in the Yates, most of the Queen producers (the Queen sands are located below the Yates) were also completed in the Yates to produce commingled from the Yates and Queen. As a result, the decline in oil production was temporarily arrested. However, after 1969, oil production steadily declined at a rate of 13.5 percent per year until it began to stabilize in 1979 due to drilling of infill and replacement wells, injection profile modifications by means of polymer treatments, and pattern tightening and realignment (Sections 3, 6, 7 and 8 were converted to 20 acre (81 x $10^3 m^2$) five spot patterns and Sections 9 and 10 to 20 acre line drive patterns).

At the end of 1988, the six sections produced 29% of the OOIP from the Yates. Relative to primary recovery, waterflooding the Yates has been very successful. This is exemplified by the 2.3 ratio of ultimate secondary to ultimate primary production from wells existing at the beginning of waterflooding. The favorable mobility ratio in this reservoir indicates good areal sweep efficiency. However, because of the high Dykstra-Parsons coefficient (0.85) and permeability contrast among the major sands, the vertical sweep efficiency is poor. Even after injecting 2.6 waterflood moveable pore volumes only 50% of the oil recoverable by waterflooding has been produced.

RESERVOIR GEOLOGY AND PROPERTIES

A comprehensive geologic study and reservoir characterization[1] was conducted for the NWE Field to characterize the individual reservoirs of the Yates which consist of very fine grained sandstones to siltstones separated by dense dolomite beds. These sands in descending order are the: A, BC, D, E, Stray, J_1 and J_2 (Figure 3). The general depositional environment was that of a tidal flat (sabkha) to lagoonal setting situated to the east of and behind the shelf margin. The reservoirs were deposited as sand and silt in the subtidal to beach environment and silt to clay in the supratidal environment. Depositional strike was parallel to the shelf margin, paralled to the present day northwest-southeast section lines. The greatest amount of reservoir homogeneity will be along those lines in the strike direction.

The BC sand, which has the largest reservoir capacity, is best described as a siltstone to fine-grained sandstone with detrital clay. The depositional environment was that of a shallow water tidal flat with an abundant amount of windblown sediments. A zone of low porosity and permeability trends northwest-southeast through the middle of the project area. Most of the BC was in the original gas cap. The D and E sands are similar to the BC. However, porosities and permeability are highly variable. The majority of the D and E sands are within the original gas cap in the eastern sections (1-5). The Stray section is composed of thin bedded, lenticular, intertidal to subtidal siltstones and fine grained sandstones with the highest clay content of any Yates interval. Because of this, permeability and reservoir continuity suffer while porosity remains high. The J_1 and J_2 sands are composed of coarser sands with much less clay content and, therefore, higher effective porosities and permeabilities. The depositional environment was that of a beach to nearshore marine where turbulence winnowed finer silts and clays out of the strike oriented sand deposits. These sands are best developed in the western sections (6-10). Average reservoir properties for the Yates are described in Table 1.

The Queen Formation which lies below the Yates is composed of intervals of fine grained sandstones to siltstones (separated by dense dolomite beds) each of which is composed of numerous thin, lenticular sands with poor lateral continuity. The Queen sands are difficult to flood and will be excluded from the CO_2 flood.

LABORATORY WORK

Extensive laboratory work was conducted to support the evaluation of CO_2 flooding in the NWE Field.

- Black oil PVT and oil-CO_2 phase behavior studies of recombined separator oil and gas samples (Table 2) to determine oil swelling (Figure 4), viscosity reduction and phase transition pressures vs. mole percent CO_2 (Figure 5).

- Slim tube experiments to determine minimum miscibility pressure (MMP) of pure CO_2 and oil (Figure 6). It was also verified that a published correlation[2] adequately estimates the MMP for NWE oil and CO_2 contaminated with hydrocarbon gases.

- CO_2 flooding of long cores (Figure 7) to determine the mobilization and recovery of the waterflood residual oil saturation.
  Floods were conducted with pure and impure CO_2 and with different WAG ratios (Table 3).

- Amott tests to determine the wettability of wettability-preserved and wettability-restored cores. The Amott index to oil was zero for all tests, suggesting that the Yates sands are water wet.

CO_2 INJECTIVITY TEST

A CO_2 injectivity test was conducted to investigate injectivity losses during CO_2 and water injection cycles[3]. An injector in good mechanical condition and with no hydraulic fracturing was selected for this purpose. Prior to, during and after CO_2 injection, step rate tests (Figure 8), injection profile surveys (Figure 3) and pressure transient falloff tests were run. After injecting 30 MMSCF ($0.85 \times 10^6 m^3$) of CO_2 (1.3% HCPV), the well was returned to water injection. The major conclusions were:

- No reduction in injection rates was observed during and after CO_2 injection. The CO_2 injection rate (expressed in terms of reservoir barrels) was about 20% higher than the water injection rate at same flowing bottom hole injection pressures.

- No significant change in injection profile was observed during and after CO_2 injection.

- The CO_2 falloff data were used to estimate parameters such as mobility ratio, swept volume and average CO_2 saturation in the swept region. Those are in good agreement with laboratory measurements from CO_2 core floods[4].

CO_2 FLOOD PERFORMANCE PREDICTIONS

Simulation Approach

The initial CO_2 flood design called for a history match of the waterflood performance of the six section project area, the selection of typical patterns including a detailed reservoir characterization, a history match of the waterflood performance, a prediction for continuation of the waterflood, and predictions for CO_2 flooding, and the scale up of the pattern predictions to the whole project area.

However, for reasons of time, computer and individual well data quality limitations, the initial design plan had to be changed to the simpler approach of average patterns. Because of the superior quality of battery-wide production and injection data (there is a battery for each section), three-dimensional pattern models were developed for four of the six sections in the project area. A minimum of ten to twelve layers were necessary to characterize the seven major sand bodies of the Yates. An areal view of the model and the layer properties for one of the models are shown in Figure 9 and Table 4, respectively. Net pay and porosity for each of the major sand bodies are averages developed from geologic maps. The permeability stratification within and among the major sand bodies was developed from core data and injection profiles. The Dykstra-Parsons coefficient for the layered model agreed with that calculated from core data.

History Matching

History matching with a finite-difference reservoir simulator was conducted by inputting the scaled oil production and water injection rates for the years 1929 to 1986 and letting the simulator calculate gas and water production rates and reservoir pressures. Due to limited GOR and pressure data, history matching consisted mostly of matching water production rates. The match was largely obtained by adjusting layer permeabilities and, to a lesser degree, the oil and water relative permeability curves (Figure 10).

To realistically predict the timing of CO_2 breakthrough at the producers, particular attention was paid to matching the water breakthrough time. In developing the average pattern model, it was assumed that most of the oil response and water breakthrough observed in the field between 1955 and 1962 came from high permeability zones. This assumption apparently is supported by the good correlation between cumulative oil and cumulative water production for individual wells during 1955-62 (Figure 11). Wells with the highest cumulative water production during this time period also had the highest cumulative oil production.

Performance Predictions - Patterns

A four-component miscible flood simulator (similar to the one described in Reference 5) was selected for the CO_2 flood predictions. This simulator is suitable for first-contact miscibility or for multiple contact miscibility if the miscibility occurs within a mixing zone the length of which is small compared to the length of the imposed grid. An oil/solvent mixing factor of 0.67 was assumed. The residual oil saturation to miscible flooding (SORM) was based on the results from CO_2 corefloods (Table 3). No waterblocking in addition to what is already reflected in the experimental SORM was introduced. The CO_2 injection rate (in terms of reservoir barrels) was increased 20% above the average water injection rates at the end of the history match. A 32% HCPV CO_2 slug was injected over 7 years at a WAG ratio of 1:1 (2.5% HCPV per WAG cycle). This was followed by reinjection of produced CO_2 for three years. In total, a 38% HCPV CO_2 slug was injected over a 10 year period. The simulation results (history match, waterflood and CO_2 flood prediction) for one of the average patterns are shown in Figure 12.

Sensitivity studies were conducted to examine the effects of changes in the following parameters on oil recovery: WAG ratio, CO_2-oil mixing parameter, vertical permeability and SORM. Continuous CO_2 injection (zero WAG ratio) recovered only 7.1% of the OOIP as compared with 9.8% with a WAG ratio of 1:1 mostly because of excessive CO_2 channeling through the high permeability layers. At a WAG ratio of 2:1, peak oil production rates were maintained for a longer time period. Incremental recovery, however, decreased to 7% OOIP because of higher SORM (SORM from the CO_2 core floods is higher for a 2:1 WAG ratio than for a 1:1 WAG ratio because of increased water blocking). Incremental oil recovery ranged from 7.4 to 10.5% OOIP for variations in CO_2-oil mixing parameter between 0.5 and 0.75. Changes in vertical permeability from zero to 10 percent of horizontal permeability within each major sand body had negligible effect on incremental oil recovery. This result was confirmed by an analytical model which expresses, as a function of vertical and horizontal solvent velocities, the horizontal distance the solvent will travel from the injector until it is concentrated in the top third of a layer. The analytical model predicts that in the high permeability layers (which are the major source for CO_2 flood oil) this separation distance is greater than the distance between injectors and producers for plausible vertical permeabilities. Over the range of SORM given in Table 3, the incremental oil recovery ranged from 6.3% to 9.8% OOIP.

Optimum Economic CO_2 Slug Size

Oil recovery predictions were made for seven CO_2 slug sizes (15% to 75% HCPV). The optimum economic slug size was found by balancing the increase in revenues from additional oil production with the cost of additional CO_2 purchased and the increasing capital and operating costs to process larger volumes of the produced CO_2. In terms of rate of return it was found that the optimum slug size lies between 38% to 60% HCPV of CO_2 injected (Figure 13).

Performance Predictions - Project Area

The CO_2 flood prediction for the entire project area (Table 5) is based on the scale up of the pattern simulation results. The scale up for the four sections for which average pattern simulations were performed is straight forward. The prediction for a given section equals the prediction from the average pattern of that section times the number of patterns to be flooded with CO_2. That is, it is simply the reverse of the scale down step that defined the average patterns. No pattern simulations were performed for Sections 9 and 10 because of their similarities in waterflood performance with Sections 8 and 7, respectively. However, since Sections 9 and 10 were converted to line drives in 1979, correction factors had to be developed before the predictions for five spot patterns could be applied. These correction factors were developed for one of the average patterns as follows:

- A line drive model was initialized with the history matched saturations and pressures from a five spot pattern as of 1979 (the year when pattern realignments and tightening were initiated in the field). The saturation and pressure values for the cells outside the area covered by the five spot model were based on symmetry considerations. Continuation of the waterflood to the start of the CO_2 flood (10 years) allowed the saturation and pressure distributions from the five spot to adjust to those found in a line drive pattern.

- Annual correction factors to convert CO_2 flood performance predictions for five spot to line drive patterns were calculated from the difference in CO_2 flood predictions for the five spot and line drive patterns (Figure 14).

Performance -- Comparison With Other Models

The performance prediction from the conventional reservoir simulation approach described in this paper was compared with the prediction from a model which combines a 4,000 cell cross-section simulation model with heterogenities described by fractal statistics with a streamtube model[6]. Results on incremental oil response were in good agreement. Both models predict poor vertical sweep and rapid CO_2 breakthrough at the producers.

CONCLUSIONS

- CO_2 flooding is expected to recover an additional 8% of the OOIP from these heterogeneous sandstone reservoirs, increasing ultimate oil recovery to 39% of OOIP.

- Gross CO_2 utilization is predicted to be high (12 MSCF/BO [2136 m^3/m^3]) because of poor vertical conformance which, given the physical condition of many of the injection wells, cannot be controlled. Net CO_2 utilization will be 4 MSCF/BO (712 m^3/m^3).

- Sensitivity studies indicate that oil recovery is quite sensitive to WAG ratios, CO_2-oil mixing factor and SORM but insensitive to variations in vertical permeability. A WAG ratio of 1:1 is optimal.

A cost effective methodology (average patterns and scale up techniques) was developed to forecast the performance of a major new CO_2 flood.

OWLEDGEMENTS

authors thank Chevron U.S.A. Inc. for permission to publish this per. They also thank R. B. Crookston for guidance, technical view, and suggestions throughout the course of this study. The aboratory work was conducted/supervised by the Fluid Analysis & Phase Behavior, the Miscible Gas, and the Fluid Flow & Rock Mechanics Sections of the Chevron Oil Field Research Company.

REFERENCES

1. Davidsen, E. K., Wylie, A. S., Gillespie and Butler, R. S.: "A Computer - Aided Geological Characterization of a Sandstone Reservoir, North Ward Estes Field, Ward and Winkler Counties, Texas"; presented at the AAPG National Convention, Houston, Texas, March 1988.

2. Sebastian, H. M., Wenger, R. S. and Renner, T. A.: "Correlation of Minimum Miscibility Pressure for Impure CO_2 Streams"; Paper SPE/DOE 12648 presented at the SPE/DOE Fourth Symposium on Enhanced Oil Recovery, Tulsa, Oklahoma, April 15-18, 1984.

3. Harvery, M. T., Shelton, J. L. and Kelm, C. H.: "Field Injectivity Experiences with Miscible Recovery Projects Using Alternate Rich Gas and Water Injection," J. Pet. Tech. (Sept. 1977), pp. 1051-55.

4. Tang, R. W. and Ambastha, A. K.: "Analysis of CO_2 Pressure Transient Data with Two and Three- Region Radial Composite Models"; Paper SPE 19275 presented at the 63rd Annual Technical Conference and Exhibition, Houston, Texas, October 2-5, 1988.

5. Todd, M. R. and Longstaff, W. J.: "The Development, Testing, and Application of a Numerical Simulator for Predicting Miscible Flood Performance," J. Pet. Tech. (July 1972), pp. 874-882.

6. Tang, R. W., Behrens, R. A. and Emanuel, A. S.: "Reservoir Studies using Geostatics to Forecast Performance"; Paper SPE 18423 presented at the 10th SPE Symposium on Reservoir Simulation, Houston, Texas, February 6-8, 1989.

Table 1
Yates Reservoir Properties (CO_2 Project Area)

FORMATION	YATES
LITHOLOGY	SANDSTONE
DEPTH	2600 FEET
RESERVOIR TEMPERATURE	83 °F
POROSITY	16 % PV
PERMEABILITY TO AIR	37 MD
DYKSTRA-PARSONS COEFFICIENT	0.85
INITIAL CONDITIONS:	
WATER SATURATION	50 % PV
RESERVOIR PRESSURE @ GOC	1400 PSIA
SATURATION PRESSURE	1400 PSIA
OIL FORMATION VOLUME FACTOR	1.2 RB/STB
OIL VISCOSITY	1.4 CP
SOLUTION GOR	500 SCF/STB
OIL GRAVITY	37 °API
RESIDUAL OIL SATURATION TO WATERFLOODING	25 % PV
MINIMUM MISCIBILITY PRESSURE (PURE CO_2)	937 PSIA
FLOOD PATTERNS (Sections 3, 6 to 8)	20 Acre FIVE SPOTS
FLOOD PATTERNS (Sections 9, 10)	20 Acre LINE DRIVES

Table 2
Analysis of Separator and Reservoir Fluids

	SEPARATOR		RESERVOIR
COMPONENT	GAS (Mole %)	LIQUID (Mole %)	FLUID (Mole %)
NITROGEN	0.44	0.00	0.19
CARBON DIOXIDE	1.25	0.03	0.44
HYDROGEN SULFIDE	1.89	0.04	0.14
METHANE	56.89	0.34	20.25
ETHANE	15.47	1.01	5.91
PROPANE	13.44	2.82	5.89
ISO-BUTANE	2.23	1.81	1.46
N-BUTANE	4.88	5.68	4.12
ISO-PENTANE	1.41	3.97	2.53
N-PENTANE	1.08	3.67	2.38
HEXANES	0.75	6.40	4.35
HEPTANES-PLUS	0.27	74.23	52.34
TOTALS	100.00	100.00	100.00

OTHER PHYSICAL PROPERTIES

BUBBLE POINT PRESSURE	870 PSIA
SOLUTION GAS @ 870 PSIA	288 SCF/STB
TEMPERATURE	83 °F
OIL VISCOSITY @ 870 PSIA	1.60 CP
MOLE WEIGHT HEPTANES-PLUS	229
DENSITY @ 60°F (HEPTANES-PLUS)	0.87

Table 3
CO_2 Core Floods

WAG RATIO	SOI (%PV)	SORW (%PV)	SORM (%PV)	INJECTION GAS COMPOSITION %CO_2	%HC GAS
0:1	57.80	29.34	14.00	100	0
1:1	57.84	29.02	11.45	100	0
1:1	58.78	29.49	13.82	88	12
2:1	58.00	29.81	17.14	100	0

Table 4
Layer Properties of One of the Average Patterns

LAYER	SAND	SOI (% PV)	SGI (% PV)	NET PAY (Feet)	POROSITY (%)	K_{x-y} (md)	K_z* (md)
1	BC (GAS)	10	41	10.0	16.6	11.0	.11
2	BC	51	0	4.8	16.3	11.0	.11
3	BC	51	0	1.3	16.3	36.8	.20
4	BC	51	0	8.8	16.3	1.0	.01
5	D&E (GAS)	10	41	5.0	16.8	10.0	.10**
6	D&E	51	0	1.6	16.8	54.0	.20
7	D&E	51	0	19.5	16.8	4.0	.04
8	STRAY	51	0	2.0	15.3	15.0	.15**
9	STRAY	51	0	11.9	15.3	2.0	.02
10	J1&J2	51	0	21.5	16.3	26.0	.20**
11	J1&J2	51	0	15.0	16.3	66.0	.20
12	J1&J2	51	0	11.0	16.3	1.5	.02

*One percent of K_{x-y} with 0.2 md maximum

**Zero transmissibility between layers 4 and 5, 7 and 8, 9 and 10

Table 5
CO_2 Flood Performance Prediction

RECOVERY TO-DATE	29%	OOIP
ULTIMATE RECOVERY (PRIM. & SEC.)	31%	OOIP
CO_2 FLOOD RECOVERY	8%	OOIP
SLUG SIZE	38%	HCPV
CO_2 Injection/WAG Cycle	2.5%	HCPV
WAG RATIO	1:1	RB/RB
CO_2 UTILIZATION		
GROSS	12	MSCF/BO
NET	4	MSCF/BO

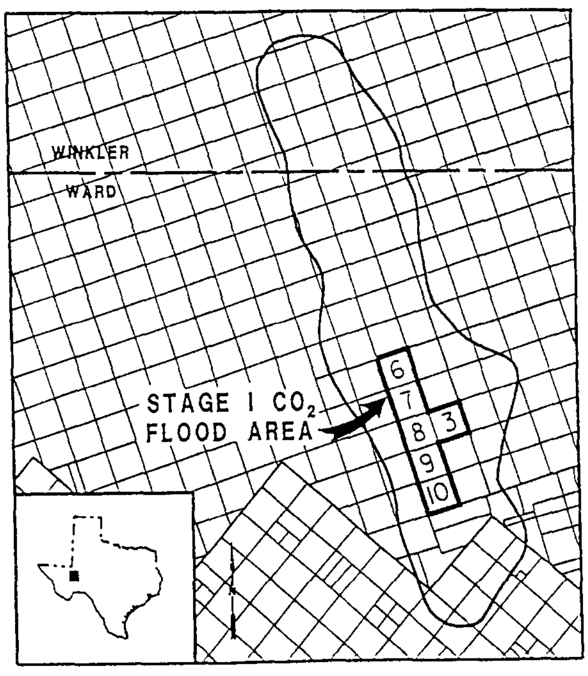

Figure 1 - North Ward Estes Field

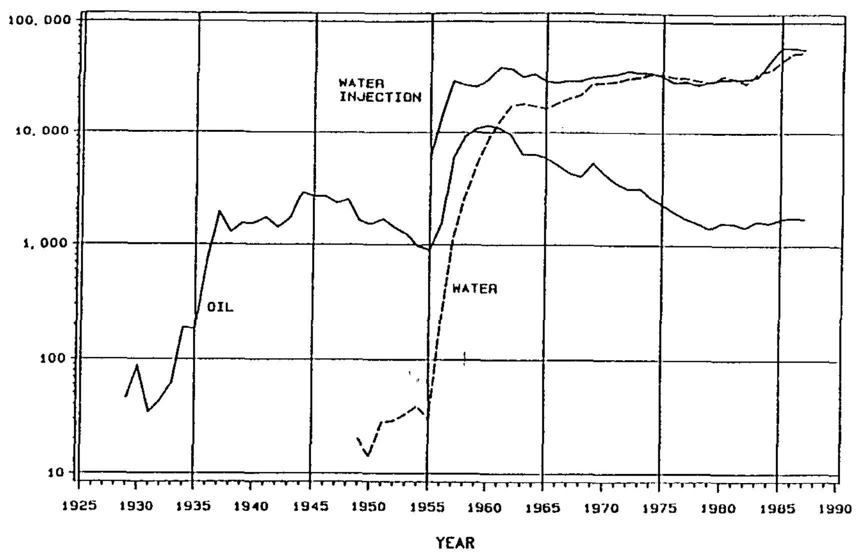

Figure 2 - Production and injection history–six-section project area

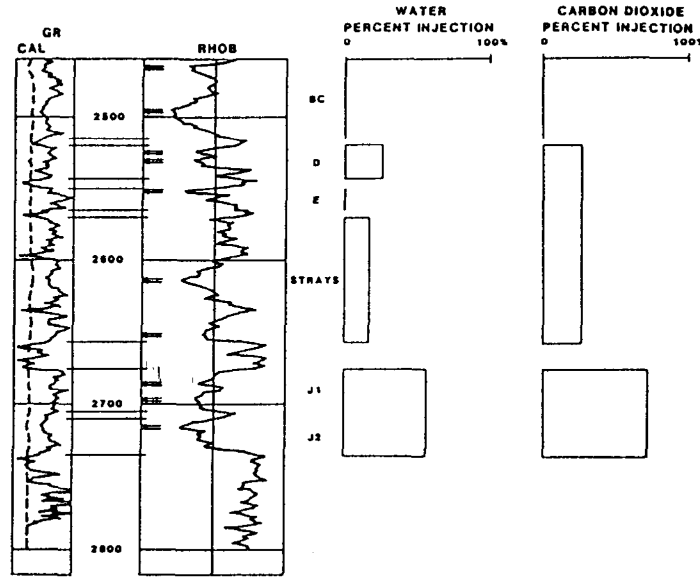

Figure 3 - Injection profile surveys

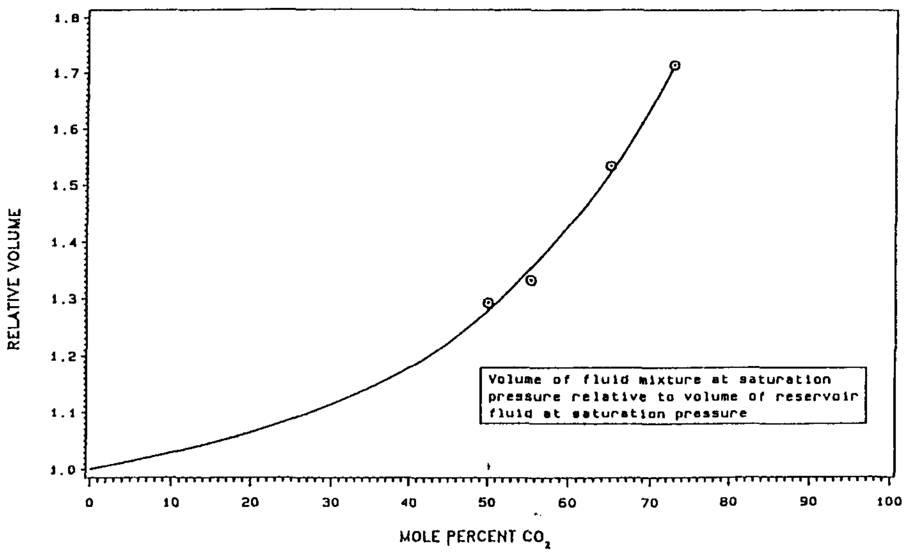

Figure 4 - Relative volume as a function of mole percent CO_2

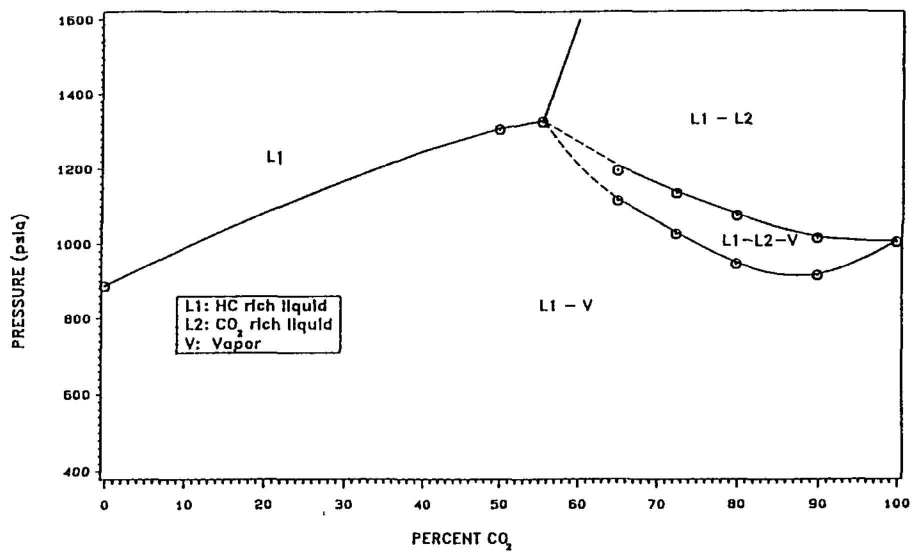

Figure 5 - Phase transition pressures vs. mole percent CO_2

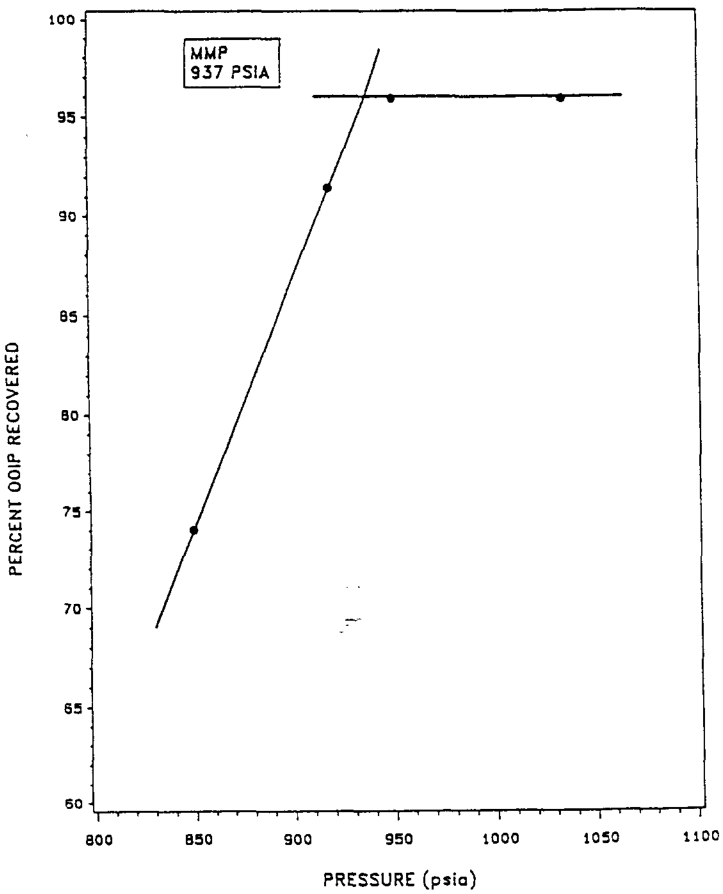

Figure 6 - Percent oil-in-place recovered vs. pressure

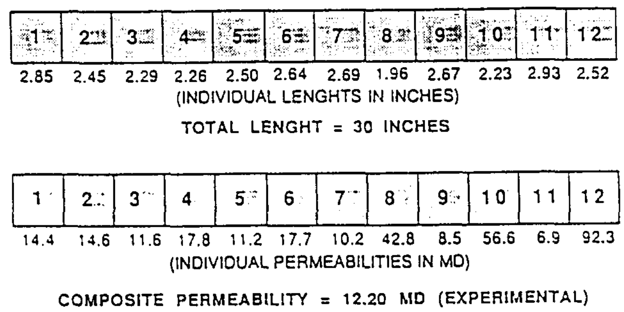

Figure 7 - Long core properties

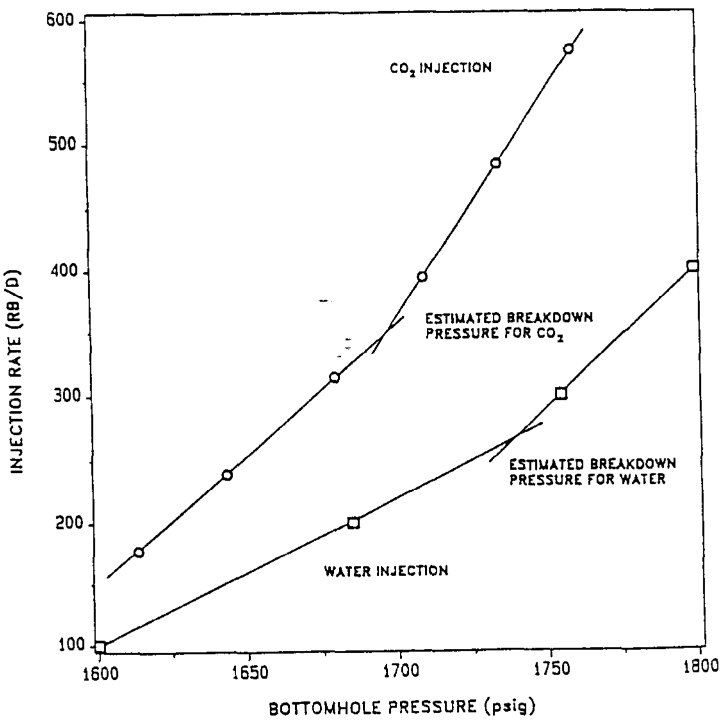

Figure 8 - Step rate tests

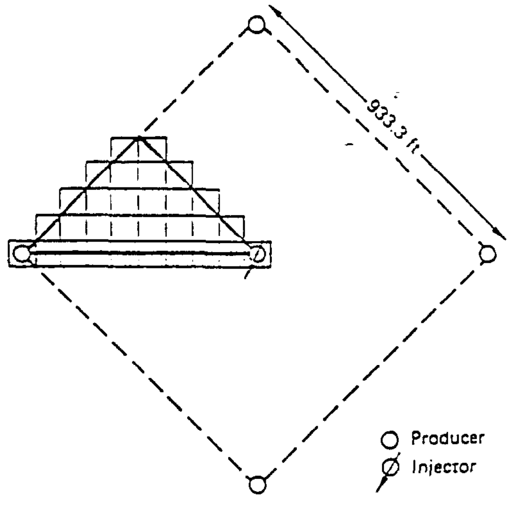

Figure 9 - Areal view of 1/8 five-spot pattern

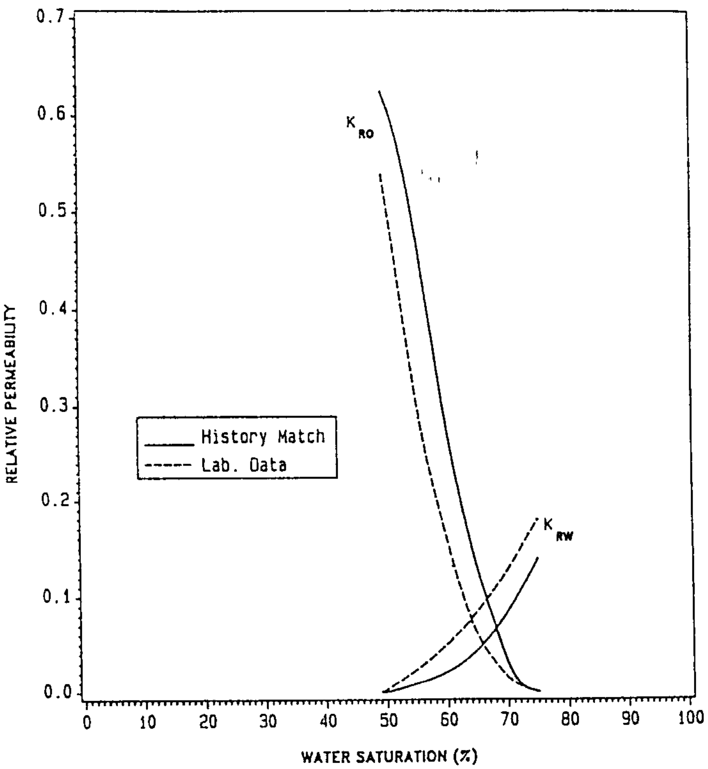

Figure 10 - Water/oil relative permeability

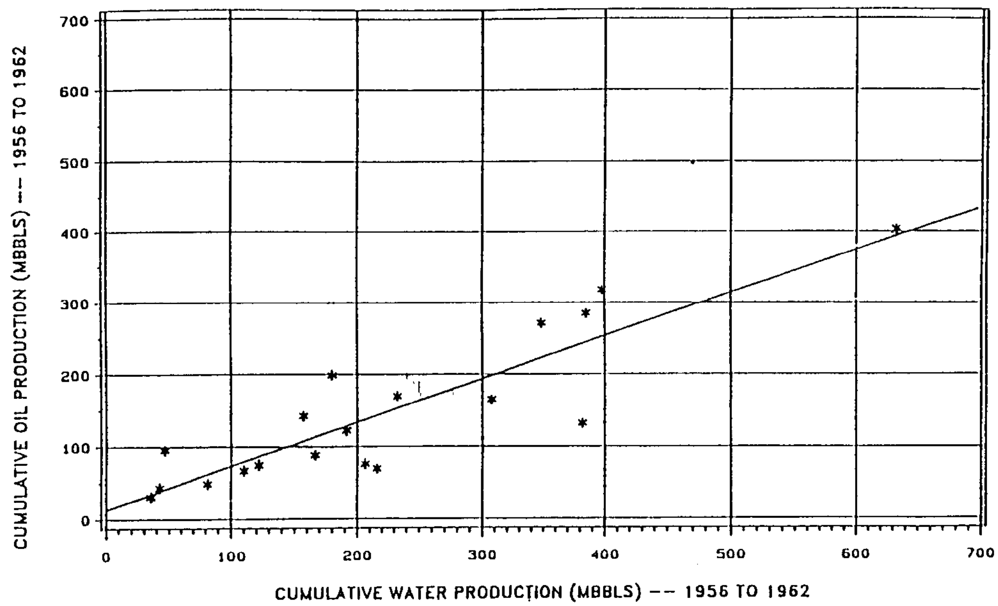

Figure 11 - Correlation for wells on 10-acre spacing (Section 7)

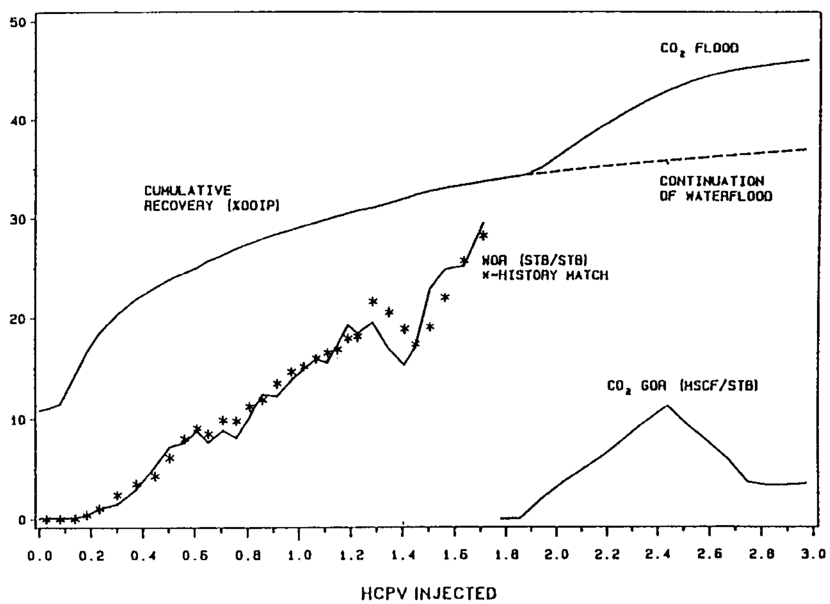

Figure 12 - Reservoir simulation results for an average pattern

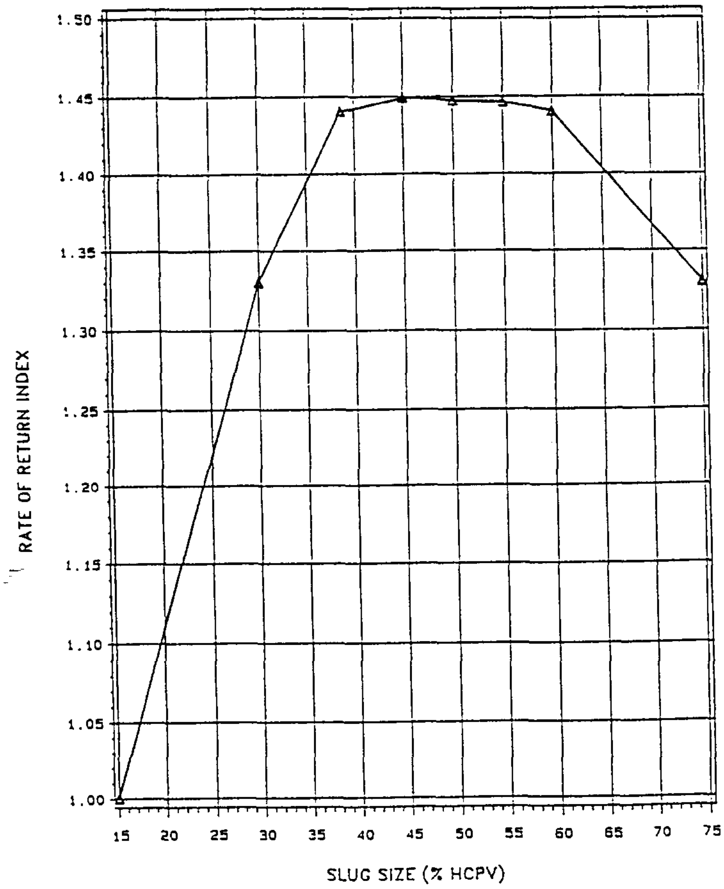

Figure 13 - Optimum CO_2 slug size

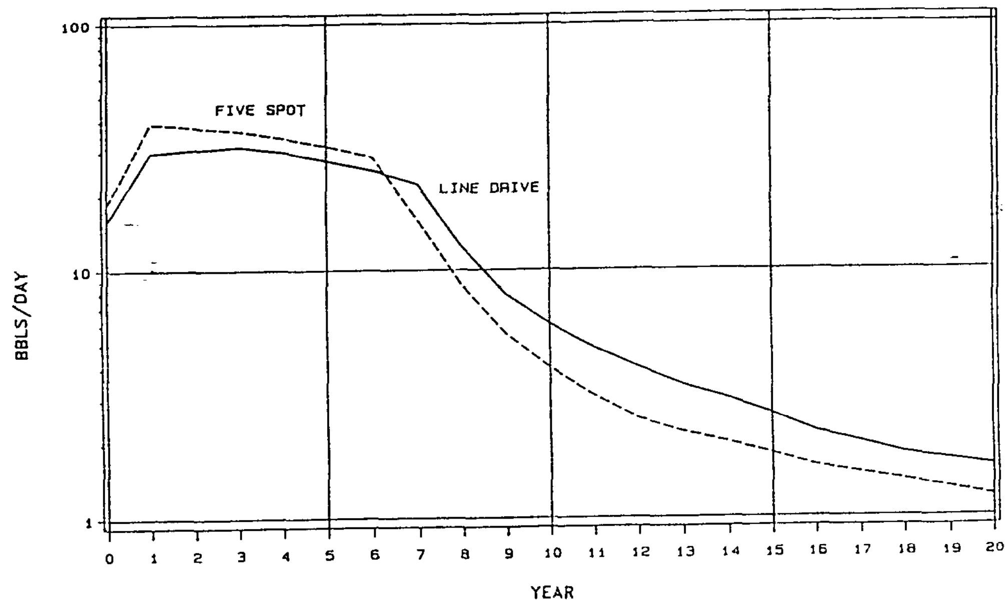

Figure 14 - Incremental oil production–line drive vs. five-spot